DOI: 10.2478/fas-2022-0004
FATIGUE OF AIRCRAFT STRUCTURES
Volume 2022: Issue 14, pp. 29-46

PREDICTION OF FATIGUE CRACKS USING GAMMA FUNCTION

Abdelfetah Moussouni*, Mustapha Benachour, Nadjia Benachour
Faculty of Technology and Science, University of Tlemcen,
BP 230 – 13000 ChetouaneTlemcen, Algeria

moussouniabdelfetah@gmail.com

Abstract

In the present study it has been endeavored to estimate the fatigue crack propagation in V-notch Charpy specimens of 2024 T351 Al-alloy. For this purpose, a new application of fatigue crack growth (FCG) is developed based on the "Gamma function." Experimental fatigue tests are conducted for stress ratios from 0.1 to 0.5 under constant amplitude loading. The empiric model depends principally on physical parameters and materials' properties in non-dimensional form. Deviation percentage, prediction ratio, and band error are used for validation of the performance of the fatigue life. The results determined from Gamma application are in good agreement with experimental FCG rates and those obtained from using Paris law.

Keywords: fatigue crack growth, stress ratio, fatigue, 2024 T351 Al-alloy, Gamma function
Article category: research article

Introduction

Fatigue crack growth (FCG) in metallic materials using fracture mechanics is expressed by the relation between the FCG rate and stress intensity factor, and it depends on other associated factors (stress ratio, amplitude loading, environment, frequency, residual stress, etc.) (Ritchie, 1999). It is identified through experimental study of FCG that the structures contain flaws either from metallurgical defects (Zerbst & Klinger, 2019) or from the damage induced during service under cyclic loading (Ritchie, 1988; Xu et al. 2017). So, the prediction of crack length requires a development of FCG models that depends on several parameters (Quan et al., 2018; Maruschak et al., 2021; Kameia & Khan, 2020; Jiang et al., 2014; Wang et al., 2019; Koyama et al., 2020) (applied cyclic loading, stress ratio, temperature, environment, and residual stress). Several FCG models have been proposed up until now for estimating the fatigue life for different materials. The first FCG model was proposed by Paris and Erdogan (Paris & Erdogan, 1963), who assumed that FCG rate "da/dN" depended on the range of stress intensity factor K where

“a” is the crack length and “N” is the number of cycles. In aluminum alloy, the exponent “m” varies between 2 and 4 (Bergner, 2001). In a study conducted by Kebir et al., a brief review of an FCG model was presented from 1963 to 2017, showing the introduction of mechanical and cyclic parameters in an FCG model. Amaro et al. have proposed a semi-empirical FCG model for the API-5L X100 pipeline steel exposed to high-pressure gaseous hydrogen. An FCG model depending on the local material behavior at specific crack locations in the heat-affected zone of 2024 T3 Al-alloy welded by Friction-stir welding (FSW) is proposed by Tzamtzis and Kermanidis. Also, some of the empirical models have been proposed for taking into account stress ratio and crack closure effect and investigated in numerous studies (Wolf, 1970; Naroozi et al., 2007; Correia et al., 2016; Borges et al., 2021; De Ioro et al., 2012). The experimental work conducted by Borges et al. showed an increase of FCG rate with the increase of stress ratio from 0.1 to 0.7 and this result indicated the existence of the crack closure phenomenon. De Iorio et al. and Grasso et al. have proposed new models for FCG that are characterized by a phenomenological similarity. These models present alternatives to the analysis technique proposed by the ASTM E647 standard. These models are robust and have shown the ability to adjust a wide range of FCG experimental data produced with different sample geometries, materials, and loading conditions. In an investigation conducted by Khelil et al., an energy-based approach has been applied to model the FCG of aluminum alloys. This approach was based on the evaluation of the new form of plastic zone (plastic radius). Li et al. have reported that the classical models developed variously by Paris and Erdogan, Forman and Mettu, and Walker cannot satisfactorily give the best prediction in the anti-fatigue design and have developed a new model together with introducing the effect of both strength and toughness. Generally, in service, the prediction of damaged components under cyclic loading can be estimated by the integration of equations of classical fatigue models. So, the direct integration becomes complicated and robust where the stress intensity factor depends on the geometrical correction $f(a/w)$ factor and crack length. The numerical integration needs different values of $f(a/w)$, which must be constant over a small increment of crack length (Hertzberg, 1996). So, to overcome this difficulty, Mohanty et al. have introduced a modern procedure to predict fatigue life by adopting an “Exponential Model” without the integration of FCGR curve under constant and variable amplitude loading. A contribution improving the exponential model has been proposed by Benachour et al. for FCG of 2024 T351 Al-alloy under applied of constant amplitude with other applied simply used by Mohanty et al. Using special function, Pawan et al. have formulate a new model named “Gamma model” based on rules exponential model for modeling a FCG in 3016L part-through cracked pipes specimens. The special function is a Gamma function correlated with non-dimensional materials’ properties (modulus of elasticity, yield strength) and fractures’ parameters (stress intensity factor, fracture toughness). In the present paper, the Gamma function is used to model FCG in V-notch Charpy specimens in four-point bending tests of 2024 T351 Al-alloy. The effect of stress ratio is also investigated.

Experimental Procedures

In this section a FCG data used in modeling process is given in others authors published papers (Benachour et al., 2015), likewise experimental details are given in the same references. Experimental fatigue tests were carried out on V-notch Charpy specimens in four-point bending tests of 2024 T351 Al-alloy extracted from a plate in T-S orientation according to the E647 ASTM standard. Specimens used in fatigue tests have square section (B × h) 10 × 10 m^2, and loaded under four points bending as shown in Figure 1a. These specimens were tested under fatigue conditions with a frequency of 10 Hz and a sinusoidal signal profile at room temperature (23ºC).

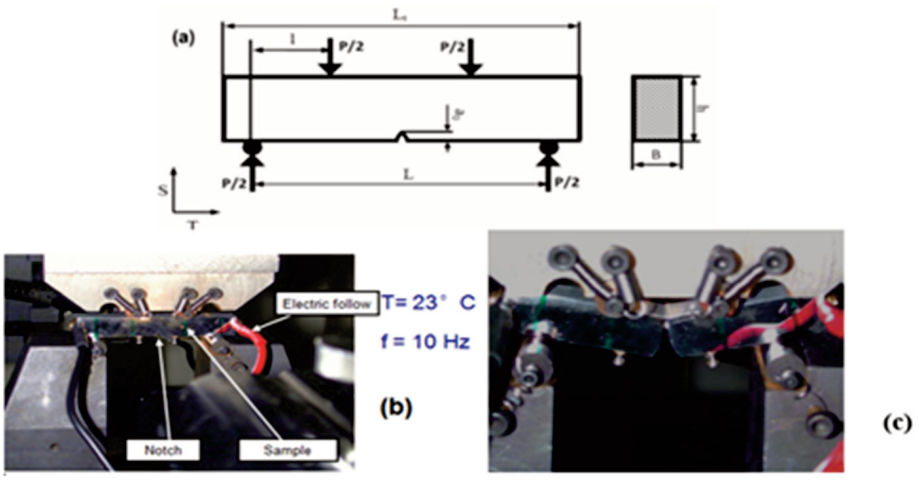

Figure 1. Four points fatigue bending tests. (a) Schematic assembly and dimensions; (b) real assembly with electrical follow; and (c) fractured specimen.

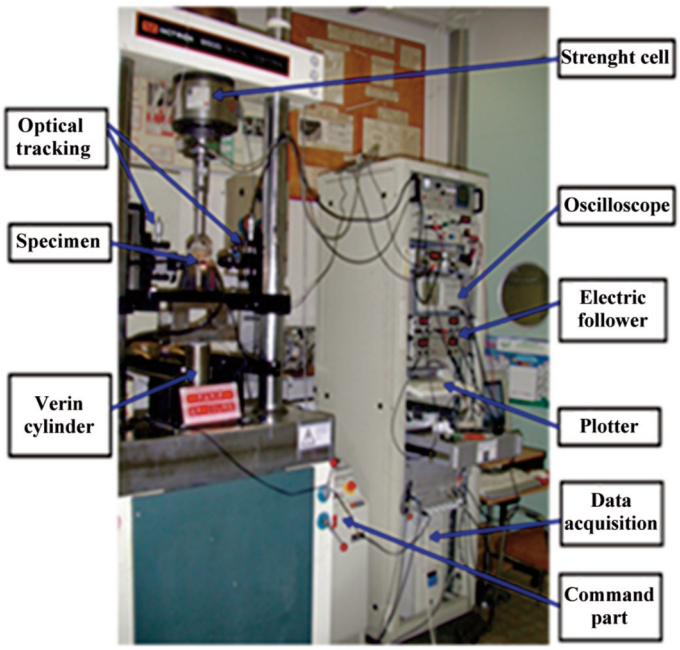

Figure 2. Servo-hydraulic machine for fatigue tests: Instron 8500.

The dimensions of specimens are given in Table 1, where the depths of notch are specified along with a notch radius of 0.20 mm. The chemical composition of Al-alloy and its mechanical properties that are used as a basis for the research conducted here have their origin in a study in the literature [29], and are detailed, respectively, in Tables 2 and 3. To determine the couple (ai, Ni), an optical micrometer with a magnification of 20× was used to measure the crack length "ai," and the respective number of cycles "Ni" is indicated in the cycle number counter (see Figure 2). The cycle number counter is placed in the Command part (Figure 2). Additionally, for measuring the length of cracks during propagation until failure (Figure 1c) using the optical micrometer, an electrical control, synchronized with the differential potentials of the sample, was used (Figure 1b).

Table 1. Dimension of fatigue specimens.

L_t	L	l	h	B	a_0
64	50	14.5	10	10	2

Table 2. Chemical composition of Al-alloy 2024 T351.

Elements	**Si**	**Fe**	**Cu**	**Mn**	**Mg**	**Cr**	**Ti**	**Zn**	**Pb**	**Ni**	**Al**
%	0.105	0.159	3.97	0.449	1.5	0.05	0.018	0.109	0.056	0.02	Rest

Table 3. Mechanical properties of Al-Alloy 2024 T351.

$\sigma_{0.2}$	σ_R	A	E	G	v
363	477	12.5	74	27.82	0.33

The stress intensity factor for this sample can be represented using the following expression [31]:

$$K = \left(3P \cdot 1 \cdot \sqrt{\pi a}\right) \Big/ \left(B \cdot h^2\right) \tag{1}$$

$f(a/h)$ presents the correction geometric function [31], which is given by the following expression:

$$f\left(a/h\right) = 14 \cdot \left(a/h\right)^4 - 13.08 \cdot \left(a/h\right)^3 + 7.33 \cdot \left(a/h\right)^2 - 1.4 \cdot \left(a/h\right) + 1.122 \tag{2}$$

and "a" is the crack length measured from the free surface of the specimens and the applied load indicated in Table 4 from initial crack length a_0 for different stress ratios. Different conditions of FCG loading, characterized by variation of stress ratio and equivalent stress intensity factors for initial and final crack length, are reported in Table 4. The experimental data and loading conditions for different stress ratios R are given in Table 4. The stress ratio "R" varies from 0.1 to 0.5. For this study, the applied maximum

load is kept approximately constant. The initial crack length "a_0" is obtained by pre-crack of the specimen under a cyclic load higher than the fatigue constant amplitude loading P.

Table 4. Experimental loading conditions and equivalents' initial and final crack lengths for different stress ratios.

R -ratio	a_0 (mm)	a_f (mm)	P_{min} (KN)	P_{max} (KN)	P (KN)	N (cycles)	ΔK_0 (MP$\sqrt{m}$)	ΔK_f (MP$\sqrt{m}$)
0.1	3.34	7.875	0.115	1.149	1.034	382.000	5.395	22.696
0.2	3.31	7.14	0.237	1.184	0.947	569.700	4.85	16.88
0.3	3.365	7.365	0.348	1.16	0.812	547.000	4.22	15.90
0.5	2.735	6.28	1.25	2.50	1.25	240.000	5.535	15.82

Experimental data, as obtained from FCG tests under different stress ratios R and used for the present application, are given in Figure 3. From these obtained results, we notice the effect of stress ratio and the effect of amplitude loading depending conjointly on applied stress ratio and the amplitude of applied load "P".

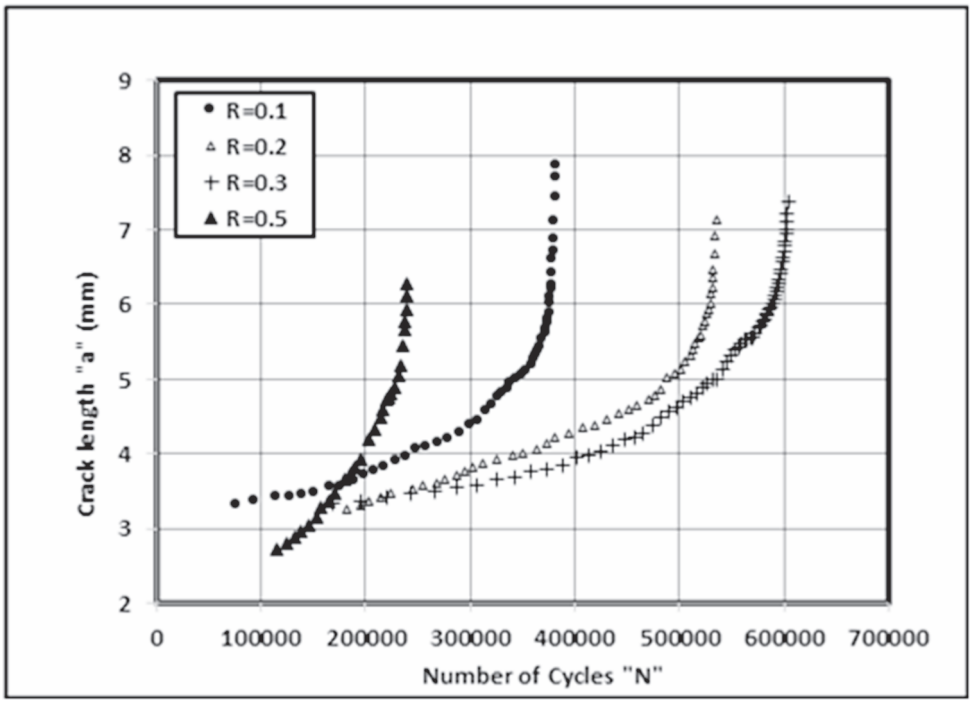

Figure 3. Experimental fatigue life of V-notch in four-point bending specimens' tests of 2024 T351 Al-alloy.

Formulation of Model

To avoid dysfunction and catastrophic failures related to the fatigue phenomenon, we have developed an empirical model of crack propagation as a function of the number of cycles using a Gamma function. The Gamma function "Γ" is a complex function, also considered as a special function. This was introduced by the Swiss mathematician Leonhard Euler in the 18th century (Chabat, 1990). For any complex number z such that Re(z) > 0, we define the Gamma function (see Eq. (3)) as the following:

$$\Gamma(z) = \int_0^{\infty} t^{z-1} e^{-1} dt \tag{3}$$

To conduct an empirical study, we would have to go through various stages. First, we modify the Gamma function with t representing the number of cycles N, and take Z as a dimensionless ratio, thus allowing the correlation of the parameters acting on the crack's growth (intrinsic, extrinsic) (see Eq. (4)):

$$\frac{m_{ij} a_j}{t} = \int_0^N N^{\left(\frac{m_{ij} a_j}{t} - 1\right)} e^N dN \tag{4}$$

Were:

$$z = \frac{m_{ij} a_j}{t} \tag{5}$$

where a_i and a_j represent crack length, t the specimen thickness, and m_{ij} the specific growth rate. The specific growth rate m_{ij} is described as an adjustable parameter of the Gamma model. Based on the previous experimental data (a-N) and using a MATLAB program, we calculate the values of m_{ij} in an incremental way at each cycle until (N) final and with a regular step 0.05 mm of the crack length (a) in order to reduce the dispersions linked to the measurements. In following the values of "m" will be correlated with the parameters which act on the propagation of the cracks representing by the factor "l" (see Eq. (6)):

$$l = \left[\left(\frac{\Delta K}{K_C} \right) \left(\frac{K_{\max}}{K_C} \right) \left(\frac{\sigma_{YS}}{E} \right) \right]^{\frac{1}{4}} \tag{6}$$

where ΔK represents the amplitude of the stress intensity factor, $K_{\max}$ the maximum of the stress intensity factor, K_C the plane stress toughness (see Eq. (7)), KIC the toughness in plane strain, E Young's modulus, and σ_{YS} the elasticity limit.

The value of the plane stress toughness K_C for the considered material is calculated from the plane strain toughness KIC from the empirical relation of Irwin (Irwin, 1967):

$$K_C^2 = K_{IC}^2\left(1+1.4\beta_{IC}^2\right) \tag{7}$$

with:

$$\beta_{IC}^2 = \frac{1}{t}\left(\frac{K_{IC}}{\sigma_{YS}}\right) \tag{8}$$

$$m_{ij} = A.l^5 + B.l^4 + C.l^3 + D.l^2 + E.l + F \tag{9}$$

A polynomial of degree 5 (see Eq. (9)) gave a better approximation of m_{ij} (l) than the polynomial of degree 3 given by Pawan et al. The values of the constants of the adjustment curves (A, B, C, D, E, and F) for different load ratios are provided in Table 5. These values of constants (A, B, C, D, E, and F) in Eq. (9) are determined using Excel code through interpolation of the values of m_{ij} in functions of the values of "l" parameters using applied polynomial equations.

Table 5. The values of the constants of the adjustment curves.

***R* -ratio**	***A***	***B***	***C***	***D***	***E***	***F***
0.1	$-44{,}955 \cdot 10^4$	$282{,}743 \cdot 10^3$	$-71{,}01 \cdot 10^3$	8932.6	−566.95	15.047
0.2	$-16{,}180 \cdot 10^4$	$139{,}644 \cdot 10^3$	$-42.59 \cdot 10^3$	6101.5	−424.49	12.113
0.3	$-10{,}975 \cdot 10^4$	$603{,}626 \cdot 10^3$	$-132.9 \cdot 10^3$	14.714	−823.39	19.20
0.5	$-56{,}762 \cdot 10^4$	$384{,}000 \cdot 10^3$	$-104.6 \cdot 10^3$	14.404	−1008.9	29.449

In the end, the length of the predicted crack is calculated from the following equation using trapeze method integrated into the MATLAB code:

$$a_j = \frac{t}{m_{ij}}\int_0^N N^{\left(\frac{m_{ij}a_j}{t}-1\right)}e^N dN \tag{10}$$

Results

The empirical model has been examined by comparing the cracking curves (a-N) of the studied material obtained from the Gamma model with the experimental results given in detail in the experimental procedures.

Figures 4–7 show the evolution of the crack length “a” as a function of the fatigue life for different stress ratios R from 0.1 to 0.5. We note that the difference between the two results is very small for the stress ratios 0.1, 0.3, and 0.5. Concerning the shift illustrated in the charge ratio 0.2 is related to the dispersions of the experimental results. It is noticed that the crack length for predicted results varies from initial to final values of experimental data with a step of 0.05 mm (see the section ‘Formulation of Model’).

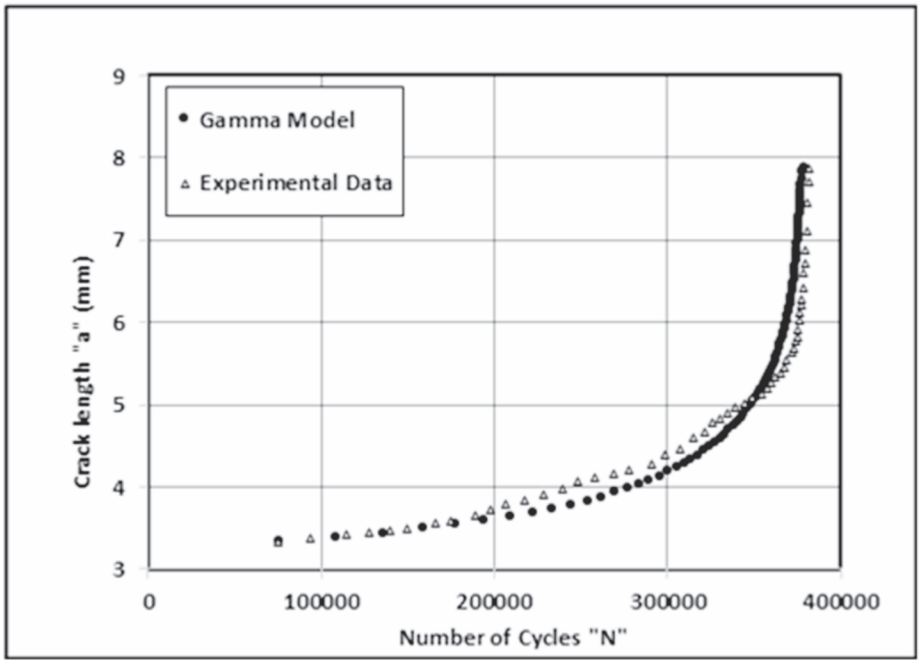

Figure 4. Comparison of predicted and experimental fatigue life at R = 0.1.

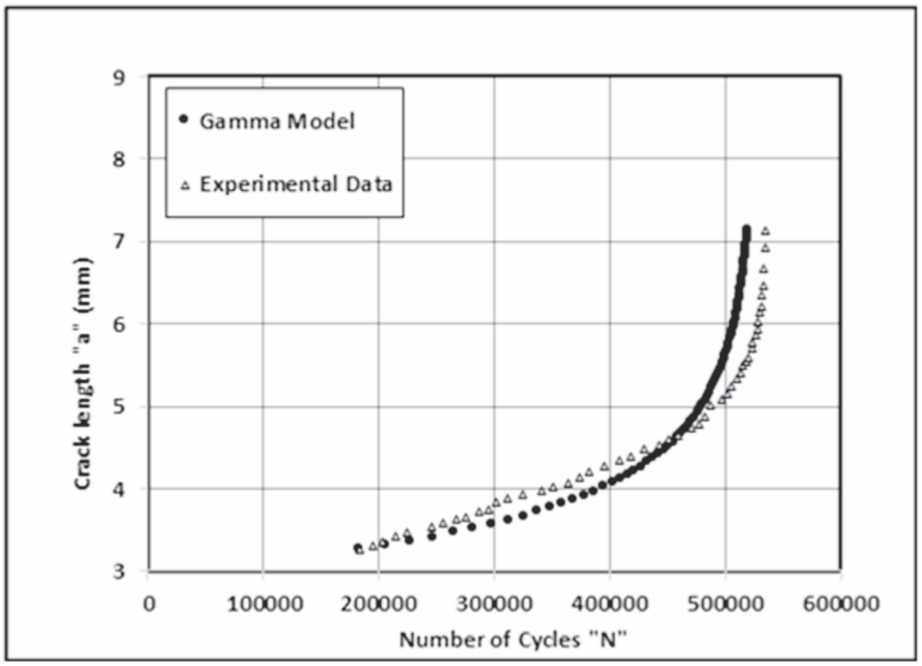

Figure 5. Comparison of predicted and experimental fatigue life at R = 0.2.

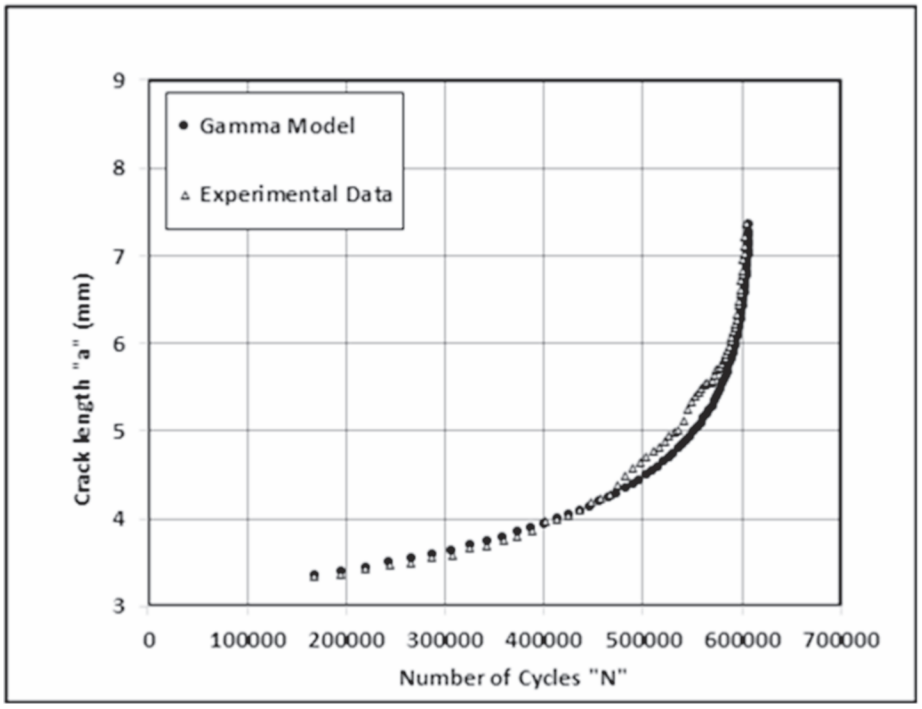

Figure 6. Comparison of predicted and experimental fatigue life at R = 0.3.

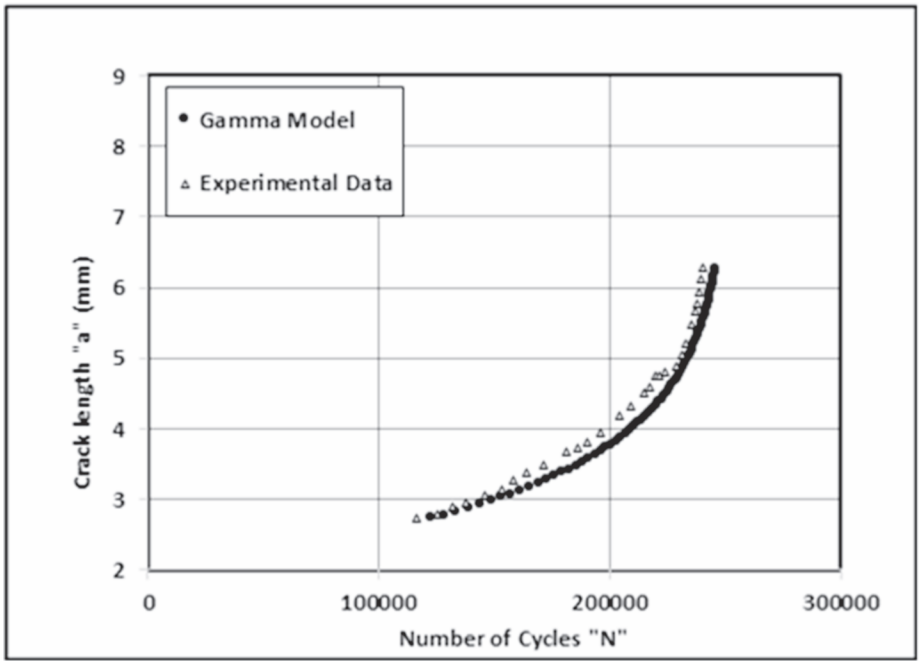

Figure 7. Comparison of predicted and experimental fatigue life at R = 0.5.

The evolution of FCG rate “da/dN” as a function of the amplitude of the stress intensity factor ΔK for different stress ratios R varying from 0.1 to 0.5 is presented in Figures 8–11, respectively. The crack growth rates are determining using secant method. The plotted results according to the Paris model [11] depending on material coefficients “m” and “C” given in Table 6, are presented and compared to the Gamma model. The coefficients “m” and “C” are determined using puissance function integrated into Excel code. The Gamma model covers Stage 2 of crack propagation well. The different curves of FCGRs are in an average position compared to the experimental values, and the proposed model gives a unique relationship of “da/dN” in function “K” and excludes the dispersions observed in experimental results.

Table 6. Coefficient of Paris model.

R-ratio	**C**	**m**
0.1	$1 \cdot 10^{-8}$	3.645
0.2	$1 \cdot 10^{-8}$	3.7053
0.3	$9 \cdot 10^{-9}$	3.8712
0.5	$5 \cdot 10^{-8}$	2.9287

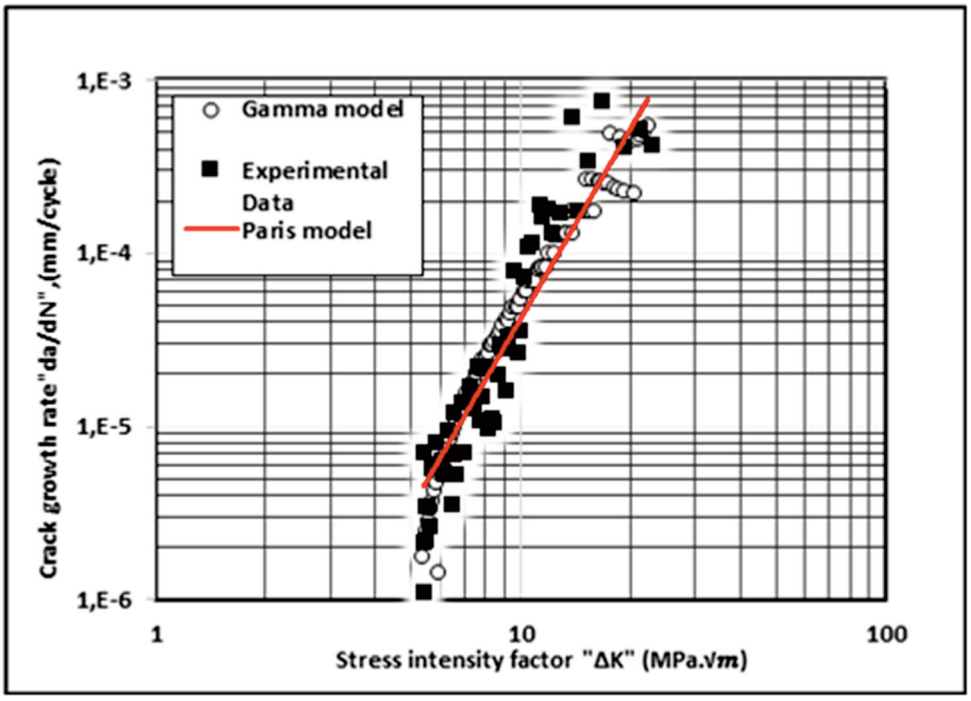

Figure 8. Comparison of predicted and experimental crack growth rate at R = 0.1.

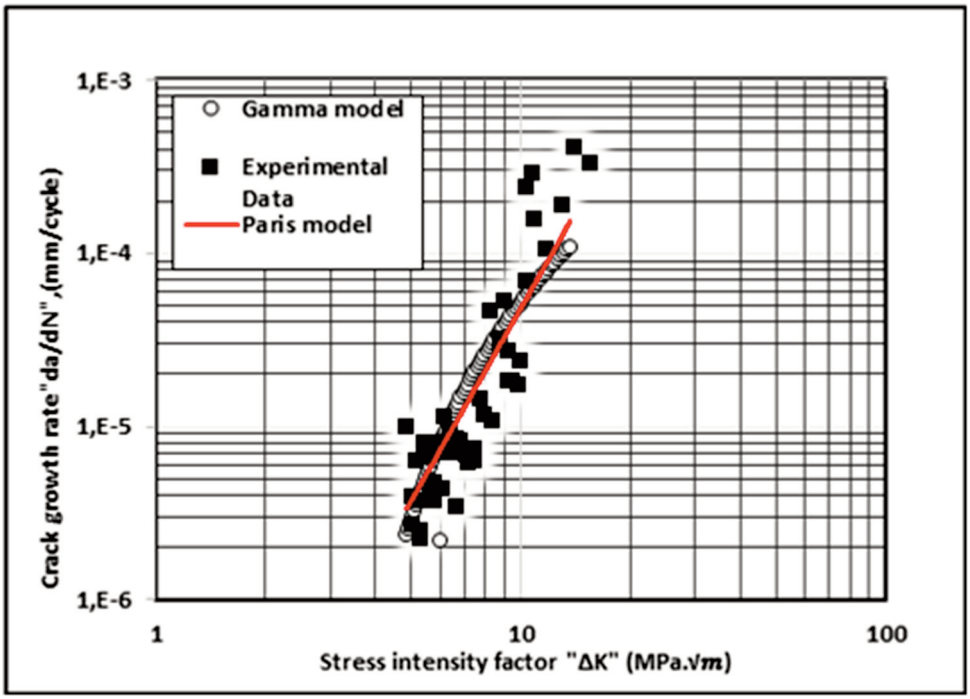

Figure 9. Comparison of predicted and experimental crack growth rate at R = 0.2.

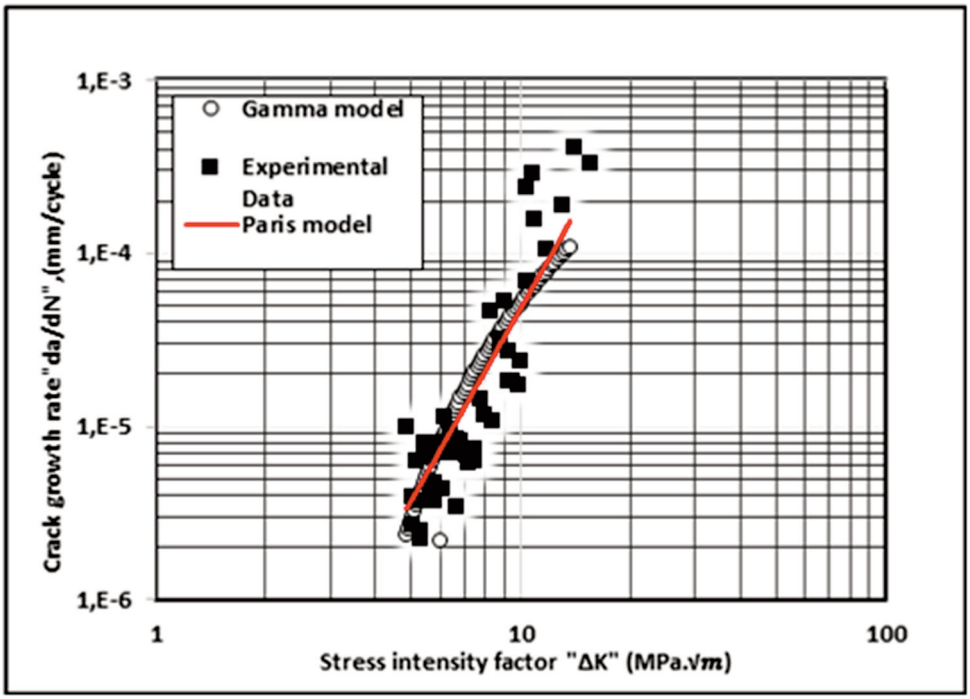

Figure 10. Comparison of predicted and experimental crack growth rate at R = 0.3.

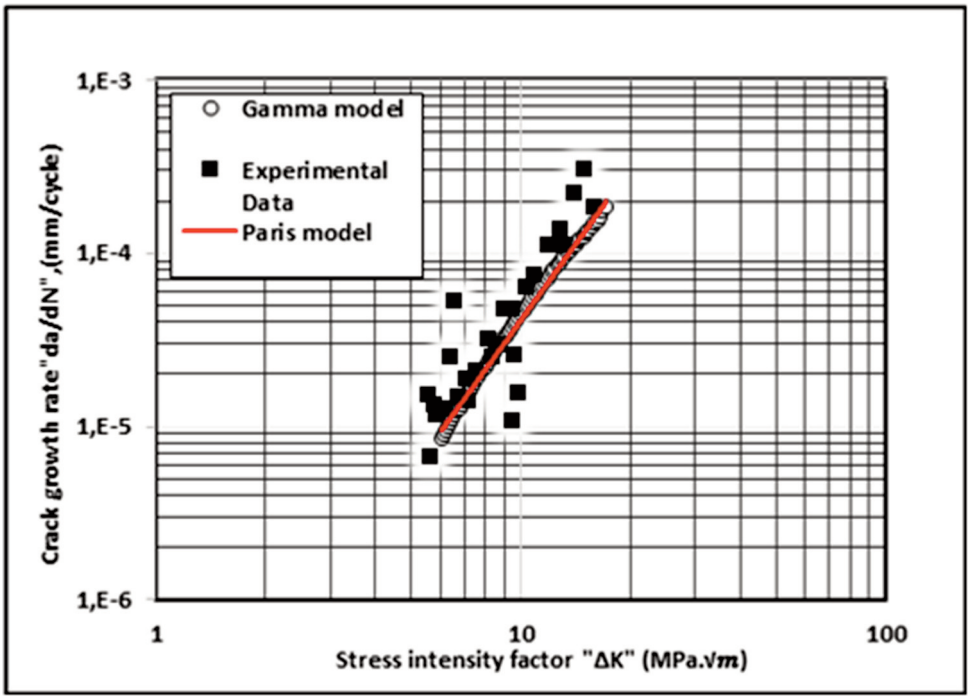

Figure 11. Comparison of predicted and experimental crack growth rate at R = 0.5.

Discussion

This part discusses the accuracy of the developed model. Once the model has been developed, it will pass to a verification phase. To facilitate a comparison between the predicted results and the experimental data, as well as to validate the performance of the developed model (Mohanty et al., 2009; Benachour et al., 2015), three criteria are used, namely deviation percentage, prediction report, and error band.

1 – Deviation percentage:

$$Dev = \frac{Predicted\ results - Experimental\ results}{Experimental\ results} \cdot 100 \qquad (11)$$

2 – Prediction report:

$$P_r = \frac{Experimental\ results}{Predicted\ results}. \qquad (12)$$

3 – Error band: defines the dispersion of the lifetime of the predicted results compared to the experimental results.

Table 7 shows the results of the first two criteria for different load ratio mean deviation percentages and the prediction ratios for the various load ratios. The average deviation equals 3.708%, and the prediction ratio is of the order of 0.967. This result is consistent with the results of Heuler et al. (1986), which show that the lifetime prediction approach is appropriate if the prediction ratio is in the interval [0.5–2].

Table 7. Performance of Gamma model

R-ratio	**0.1**	**0.2**	**0.3**	**0.5**	**Mean value**
%Dev	4.520	3.892	1.220	5.200	3.708
Prediction ratio	0.961	0.968	0.988	0.951	0.967

Figures 12–15 illustrate the results of the third criterion for various load ratios. It should be noted that the results for the studied alloy 2024 T351 vary from the interval 2% to 6%. The predicted results of fatigue life are determined for a fixed crack length obtained from the experimental specified fatigue life. It is noticed from all figures (Figures 11–14) that the scatter band is reduced with increasing the numbers of the same reported points.

The errors of the dispersion bands for the studied alloy are of the same order of magnitude compared to the results obtained on the aluminum alloys 2024 T3 and 7020 T7 in the research of Mohanty. The dispersion bands are of the order of 2.5%–5% and 2.5%–8%, respectively, for the 7020 T7 and 2024 T3 alloys for a stress ratio R = 0.1.

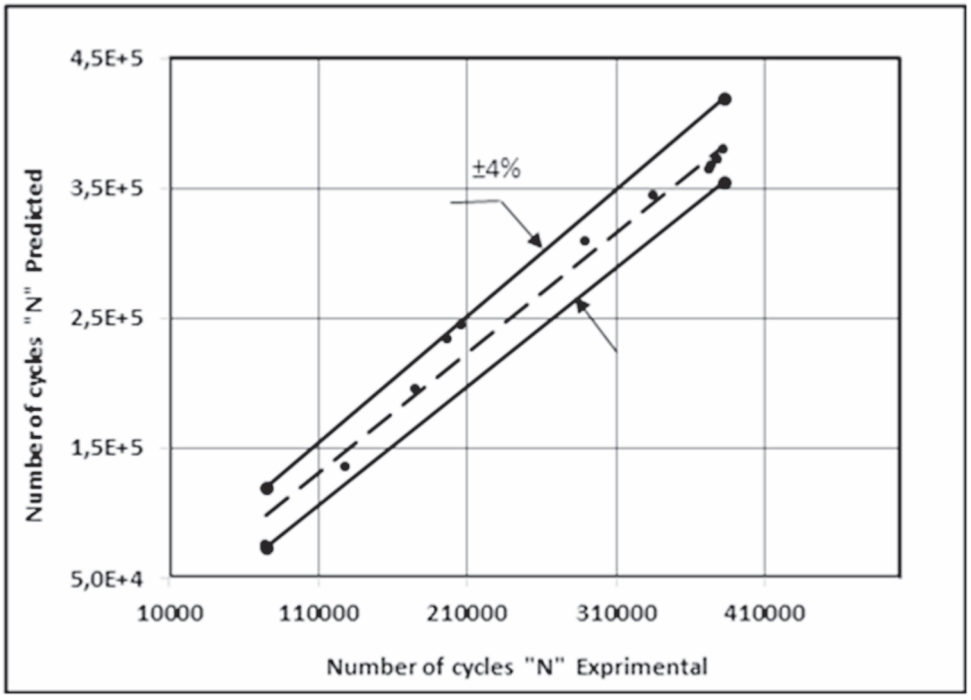

Figure 12. Error band scatter of predicted life at R = 0.1.

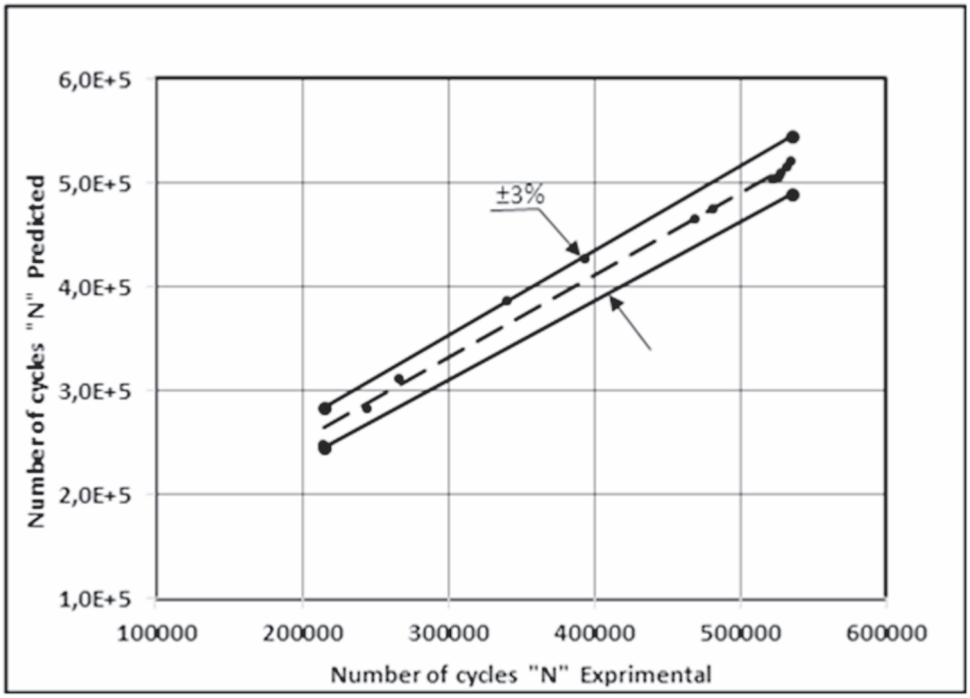

Figure 13. Error band scatter of predicted life for at R = 0.2.

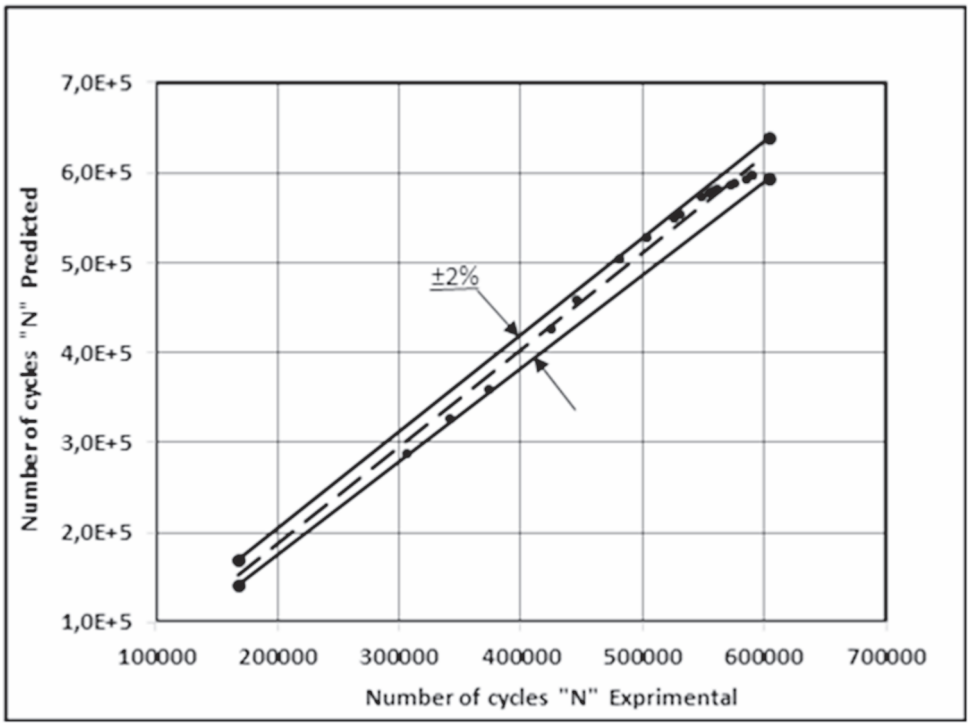

Figure 14. Error band scatter of predicted life at R = 0.3.

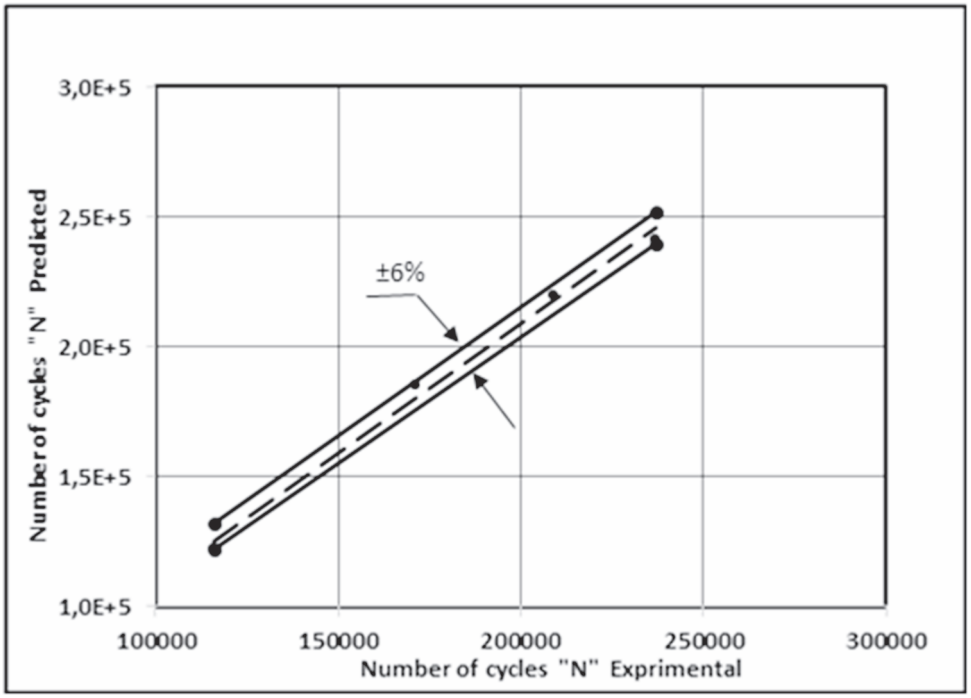

Figure 15. Error band scatter of predicted life at R = 0.5.

Conclusions

In this work, it has been determined that a special function, named "Gamma function" in the present context, can be used to determine the FCG without going through numerical integration. The experimental FCG data of 2024 Al-alloy are used for the present application under the variation of stress ratio from 0.1 to 0.5. The following conclusions can be drawn from this investigation:

- Fatigue crack propagation under constant loading in cracked V-notch Charpy specimens can be studied effectively using the Gamma function.
- The rate of the specified growth "m_{ij}" is expressed as a function of non-dimensional mechanical properties parameters and fracture parameters.
- Gamma model usage makes it accessible to emancipate the extension of the crack in corresponding with the given data about the number of cycles, or to predict the number of cycles required for a given crack extension.
- The numerical model proposed in this investigation is compared with the experimental results and the Paris Law. The results indicate that the model has been demonstrated to be in good agreement with the experimental and analytical results.
- For various stress ratios, the predicted results concerning the number of cycles vary from 2% to 6% in comparison with the experimental results.

References

Amaro, R. L., Rustagi, N., Findley, K. O., Drexler, E. S., & Slifka, A. J. (2014). Modeling the fatigue crack growth of X100 pipeline steel in gaseous hydrogen. *International Journal of Fatigue*, *59*, 262–271. https://doi.org/10.1016/j.ijfatigue.2013.08.010.

Benachour, M., Belmokhtar, A., Benchour, N., & Benguediab, M. (2015). Enhanced Exponential Fatigue Crack Growth Model for Al-alloy. *AASCIT Journal of Materials*, *1*(3), 57–63.

Bergner, F. (2001). The material-dependent variability of fatigue crack growth rates of aluminium alloys in the Paris regime. *International Journal of Fatigue*, *23*(5), 383–394. https://doi.org/10.1016/s0142-1123(01)00006-8

Borges, M. F., Lopez-Crespo, P., Antunes, F. V., Moreno, B., Prates, P., Camas, D., & Neto, D. M. (2021). Fatigue crack propagation analysis in 2024-T351 aluminium alloy using nonlinear parameters. *International Journal of Fatigue*, 153, 106478. https://doi.org/10.1016/j.ijfatigue.2021.106478

Correia, J. A. F. O., De Jesus, A. M. P., Moreira, P. M. G. P., & Tavares, P. J. S. (2016). Crack Closure Effects on Fatigue Crack Propagation Rates: Application of a Proposed Theoretical Model. *Advances in Materials Science and Engineering*, *2016*, 1–11. https://doi.org/10.1155/2016/3026745

Chabat, C. (1990). *Introduction à l'analyse complexe*. Tome 1 : Fonctions d'une variable. Éditions Mir Moscou.

De Iorio, A., Grasso, M., Penta, F., & Pucillo, G. P. (2012). A three-parameter model for fatigue crack growth data analysis. *Frattura ed Integrità Strutturale*, *6*(21), 21–29. https://doi.org/10.3221/igf-esis.21.03

Forman R.G., & Metto, S.R. (1990). Behavior of surface and corner cracks subjected to tensile and bending loads in Ti-6A1-4V alloy. National Aeronautics and Space Administration, Lyndon B. Johnson Space Center.

Grasso, M., Penta, F., Pinto, P., & Pucillo, G. P. (2013). A four-parameters model for fatigue crack growth data analysis. *Frattura ed Integrità Strutturale*, *7*(26), 69–79. https://doi.org/10.3221/igf-esis.26.08

Hertzberg, R. W. (1996). *Deformation and fracture mechanics of engineering materials* (Edition 4). J. Wiley & Sons.

Heuler, P., & Schütz, W. (1986). Assessment of concepts for Fatigue Crack initiation and propagation life prediction. *Materialwissenschaft und Werkstofftechnik*, *17*(11), 397–405. https://doi.org/10.1002/mawe.19860171105

Irwin, G.R., Kraft, J.M., Paris, P.C., & Wells, A.A. (1967). Basic Aspects of Crack Growth and Fractore. NLR Report 6598. November 21, 1967.

Jiang, S., Zhang, W., Li, X., & Sun, F. (2014). An Analytical Model for Fatigue Crack Propagation Prediction with Overload Effect. *Mathematical Problems in Engineering*, *2014*, 1–9. https://doi.org/10.1155/2014/713678

Kameia, K., & Khan, M. A. (2020). Influence of Temperature on Fatigue Crack Growth and Structural Dynamics. *TESConf 2020 – 9th International Conference on Through-life Engineering Services*. http://dx.doi.org/10.2139/ssrn.3717712.

Kebir, T., Benguediab, M., & Abdellatif, I. (2017). Influence of the variability of the elastics properties on plastic zone and fatigue crack growth. *Mechanics and Mechanical Engineering*, *21*(4), 919–934.

Khelil, F., Aour, B., Belhouari, M., & Benseddiq, N. (2013). Modeling of Fatigue Crack Propagation in Aluminum Alloys Using an Energy Based Approach. *Engineering, Technology & Applied Science Research*, *3*(4), 488–496. https://doi.org/10.48084/etasr.329

Koyama, M., Eguchi, T., & Tsuzaki, K. (2021). Fatigue Crack Growth at Different Frequencies and Temperatures in an Fe-based Metastable High-entropy Alloy. *ISIJ International*, *61*(2), 641–647. https://doi.org/10.2355/isijinternational.isijint-2020-504

Li, H. F., Zhang, P., Wang, B., & Zhang, Z. F. (2022). Predictive fatigue crack growth law of high-strength steels. *Journal of Materials Science & Technology*, 100, 46–50. https://doi.org/10.1016/j.jmst.2021.04.042

Maruschak, P., Vorobel, R., Student, O., Ivasenko, I., Krechkovska, H., Berehulyak, O., Mandziy, T., Svirska, L., & Prentkovskis, O. (2021). Estimation of Fatigue Crack Growth Rate in Heat-Resistant Steel by Processing of Digital Images of Fracture Surfaces. *Metals*, *11*(11), 1776. https://doi.org/10.3390/met11111776

Mohanty, J., Verma, B., & Ray, P. (2009). Prediction of fatigue crack growth and residual life using an exponential model: Part I (constant amplitude loading). *International Journal of Fatigue*, *31*(3), 418–424. https://doi.org/10.1016/j.ijfatigue.2008.07.015

Mohanty, J. R., Verma, B. B., & Ray, P. K. (2009a). Prediction of fatigue life with interspersed mode-I and mixed-mode (I and II) overloads by an exponential model: Extensions and improvements. *Engineering Fracture Mechanics*, *76*(3), 454–468. https://doi.org/10.1016/j.engfracmech.2008.12.001.

Noroozi, A., Glinka, G., & Lambert, S. (2007). A study of the stress ratio effects on fatigue crack growth using the unified two-parameter fatigue crack growth driving force. *International Journal of Fatigue*, *29*(9-11), 1616–1633. https://doi.org/10.1016/j.ijfatigue.2006.12.008

Paris, P., & Erdogan, F. (1963). A Critical Analysis of Crack Propagation Laws. *Journal of Basic Engineering*, *85*(4), 528–533. https://doi.org/10.1115/1.3656900

Pawan, K., Vaneshwar, K., Ray, P.K., & Verma, B.B. (2016). Modelling of Fatigue Crack Propagation in Part-Through Cracked Pipes Using Gamma Function. Mechanics, *Materials Science & Engineering*, *6*(2016). https://doi.org/10.13140/RG.2.2.16973.03043.

Quan, H., Alderliesten, R. C., & Benedictus, R. (2018). The stress ratio effect on plastic dissipation during fatigue crack growth. MATEC Web of Conferences, 165, 13002. https://doi.org/10.1051/matecconf/201816513002

Ritchie, R. O. (1988). Mechanisms of fatigue crack propagation in metals, ceramics and composites: Role of crack tip shielding. *Materials Science and Engineering: A*, *103*(1), 15–28. https://doi.org/10.1016/0025-5416(88)90547-2

Ritchie, R. O. (1999). Mechanisms of fatigue-crack propagation in ductile and brittle solids. *International Journal of Fracture*, *100*(1), 55–83. https://doi.org/10.1023/a:1018655917051

Tada, H., Paris P.C., & Irwin, G.R. (1973). *The stress analysis of cracks handbook*, 3rd ed. Del Research Corporation, Hellertown, Pensylvania.

Tzamtzis, A., & Kermanidis, A. T. (2015). Fatigue crack growth prediction in 2xxx AA with friction stir weld HAZ properties. *Frattura ed Integrità Strutturale*, *10*(35), 396–404. https://doi.org/10.3221/igf-esis.35.45

Walker, K. (b. d.). The Effect of Stress Ratio During Crack Propagation and Fatigue for 2024-T3 and 7075-T6 Aluminum. In: Effects of Environment and Complex Load History on Fatigue Life (s. 1–1–14). ASTM International. https://doi.org/10.1520/stp32032s

Wang, Y., Charbal, A., Hild, F., Roux, S., & Vincent, L. (2019). Crack initiation and propagation under thermal fatigue of austenitic stainless steel. *International Journal of Fatigue*, *124*, 149–166. https://doi.org/10.1016/j.ijfatigue.2019.02.036

Wolf, E. (1970). Fatigue crack closure under cyclic tension. *Engineering Fracture Mechanics*, *2*(1), 37–45. https://doi.org/10.1016/0013-7944(70)90028-7

Xu, L., Yu, X., Hui, L., & Zhou, S. (2017). Fatigue life prediction of aviation aluminium alloy based on quantitative pre-corrosion damage analysis. *Transactions of Nonferrous Metals Society of China*, *27*(6), 1353–1362. https://doi.org/10.1016/s1003-6326(17)60156-0

Zerbst, U., & Klinger, C. (2019). Material defects as cause for the fatigue failure of metallic components. *International Journal of Fatigue*, *127*, 312–323. https://doi.org/10.1016/j.ijfatigue.2019.06.024